

# Seismic Demand and Capacity Evaluation of Rectangular Concrete-Filled Steel Tube (RCFT) Members and Frames

C. Tort

*Graduate Research Assistant, University of Minnesota, Minneapolis, MN, USA*

J.F. Hajjar

*Professor, University of Illinois at Urbana Champaign, Urbana, IL, USA*

**ABSTRACT:** This paper presents analysis tools to be used in quantifying the demand and capacity of composite frames composed of rectangular concrete-filled steel tube (RCFT) columns and steel girders. Worldwide experimental research on RCFT members were consolidated into a database. The experimental results stored in the database were used to quantify the capacity of RCFT members at multiple levels of loading, which in turn were identified based on the local damage levels reported during the tests. A three-dimensional (3D) fully nonlinear mixed fiber finite element formulation was developed to simulate the cyclic load-deformation response of RCFT members as part of composite frames. The formulation has the capability to account for slip displacement between the steel tube and concrete core, as well as all key cyclic phenomena in the steel and concrete critical to capturing the composite characteristics of RCFT members.

## 1 INTRODUCTION

Following the successful application of Performance-Based Design (PBD) principles within a reliability framework for steel moment resisting frames (Yun et al., 2002), researchers are now seeking ways to adopt reliability-based PBD concepts in other types of structures (Moehle & Deierlein, 2004). These efforts can be realized by exploring the components of PBD (e.g., intensity measures, engineering demand parameters, damage measures and decision variables) for the structure types being studied so as to develop appropriate PBD guidelines. In this research, we are developing comprehensive analysis tools suitable for use in quantifying demand and capacity of moment-resisting frame structures composed of rectangular concrete filled tube (RCFT) beam-columns and steel girders. The analysis methods presented in this work are also appropriate to examine the components of PBD and reevaluate them to account for the characteristic features that are specific to composite structures.

RCFTs are known for their superior seismic resistance and economy due to the interaction between steel tube and concrete core (Hajjar, 2000). They are becoming increasingly popular in moment-resisting and braced frames of high-rise buildings (Morino et al., 2001, MacRae et al., 2004). It is believed that developing reliability-based PBD guidelines spreads the use of RCFT members in seismic regions.

In this research, experimental results of RCFT members available in the literature were reviewed

and documented in a comprehensive database. The information acquired from the experiments was utilized in formulating empirical damage function equations to compute the capacity of RCFT members at various performance levels. In order to extend the capacity calculations of individual members to the global level and also to determine the load and deformation demands on RCFT members and frames under seismic loads, a geometrically nonlinear distributed plasticity fiber element was derived based upon use of a mixed finite element formulation.

## 2 DEVELOPMENT OF EXPERIMENTAL DATABASE

In order to document the experimental response of RCFT members and frames, worldwide experimental tests were examined and grouped into different categories that included columns, beam-columns, panel-zones, pinned-connections, moment connections, and frames (Tort & Hajjar, 2004). The database included 364 monotonically loaded experiments and 109 cyclically loaded experiments, including comprehensive coverage of all experiments that have been reported in detail in the literature; the majority of the specimens were columns and beam-columns. The documentation of the experimental tests in the database was performed by collecting information related to the geometry, material properties, boundary conditions, loading schemes, and failure modes of the specimens. In ad-

dition, detailed information related to the local damage states of the specimens were recorded in the database with their load and deformation values from the applied loading history.

The damage experienced by RCFT members was quantified through the use of displacement-based and energy-based damage functions that documented the damage relative to the peak strength and ultimate deformation attained in the specimen. These damage functions were evaluated for each specimen in the database at each available local damage level (e.g., concrete cracking, yielding of steel tube, local buckling etc.). The damage function values were then correlated to the structural parameters of the specimens (e.g., compressive strength of the concrete, yield strength of the steel tube, depth-to-thickness ratio, etc.). For each category of RCFT specimens, this process was repeated to yield different sets of damage function equations to quantify damage at all the available local damage levels. As an example, Equation (1) shows the deformation-based damage function ( $\hat{D}$ ) of monotonically loaded beam-columns in double curvature for the local damage state of yielding of the tension flange, correlated to the parameters of the axial force ratio ( $P/P_o$ ) and the steel tube strength ratio ( $P_s/P_o$ ).

$$\hat{D} = \frac{d_{ty}}{d_o} = 1.47 \frac{P}{P_o} - 5.28 \frac{P_s}{P_o} + 3.85 \quad (1)$$

where  $d_{ty}$  is the deformation at yielding of the tension flange;  $d_o$  is the deformation when peak load is attained,  $P$  is the internal compressive axial force;  $P_s$  is the steel tube cross section axial strength; and  $P_o$  is the cross section axial strength. A parametric study was then conducted by generating multiple specimens having a wide range of material and geometric properties. The damage function equations were evaluated for each of these specimens at every local damage level. Based on the range of damage function values that resulted, the local damage levels were correlated into performance levels for each category of RCFTs. Local damage levels having energy-based damage function values ( $\hat{E}$ ) in the intervals of 0.0-0.30, 0.30-0.60, 0.60-0.95, and  $>0.95$  were mapped into Immediate Occupancy, Life Safety, Near Collapse, and Collapse Prevention performance levels, respectively. This also allowed direct comparison of the intricate interaction that occurs between the local damage levels in a composite RCFT specimen depending on the characteristics of the RCFT. For example, Figure 1 illustrates local damage level, performance level and displacement-ductility relationship obtained from the parametric study conducted for 16 beam-column specimens. It can be seen that yielding of the compression flange (YCF) is often the earliest damage level taking place while local buckling of the steel tube web (LBW) ini-

tiates at the latest stages of the loading history. Figure 1 also shows that for the specimens having high ductility ratios, yielding of the tension flange (YTF) takes place prior to local buckling of the compression flange (LBF). On the other hand, for the specimens having lower levels of ductility ratios, local buckling of the compression flange occurs earlier than yielding of the tension flange.

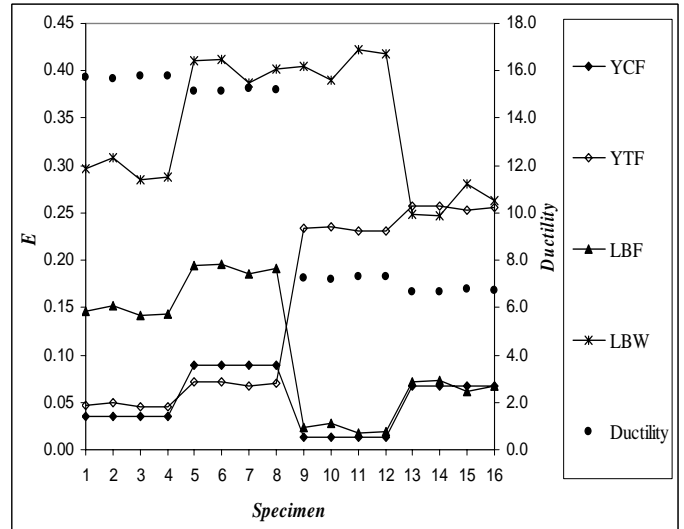


Figure 1. Comparison of energy-based damage indices for monotonically-loaded beam-column tests

### 3 DEVELOPMENT OF FINITE ELEMENT MODEL OF RCFT BEAM-COLUMNS

A fiber-based distributed plasticity finite element formulation was adopted in this research to model RCFT beam-columns. In fiber-based finite element models, the element cross-sections are divided into individual steel and concrete fibers. Throughout the analysis, stress vs. strain response of each fiber is monitored at each integration point along the element length. This allows a wide range of engineering demand parameters to be quantified based on the analysis results. For example, with the use of a fiber-based finite element formulation, it is possible to examine force-deformation response of elements, moment-curvature response of element cross-sections, and stress-strain response of individual fibers. Therefore, it is feasible to detect the engineering demand parameter exhibiting the best correlation with the intensity measure of interest. Combined with the local damage assessment study presented earlier, it is possible to correlate engineering demand parameters from the analysis results with various damage measures, performance levels, or both.

An 18 degree-of-freedom (DOF) beam-finite element was derived based on the work of Hajjar et al. (1998). In this formulation, the translational DOFs of the steel tube and concrete core were defined independently to simulate slip behavior that is typical for composite members. This resulted in 9 DOFs at each joint framed by an RCFT member. Since the

concrete core is placed inside the steel tube, the shear translational DOFs and rotational DOFs of the steel tube and concrete core were assumed to be equal to each other. Penalty functions were then utilized to keep the shear translations of the steel tube and concrete core to be the same. Therefore, differential movement between the steel tube and concrete core was allowed only in the axial direction for an RCFT oriented arbitrarily in 3D space. At an RCFT joint, the first three DOFs were assumed to be steel translations, the next three DOFs were defined as the steel tube and concrete rotations, and the last three DOFs were taken as concrete translations. This numbering scheme was selected so that when RCFT members are used as columns of a composite frame, steel girders can frame into the first six DOFs of RCFT columns. In this research, the finite element formulation proposed by Hajjar & Schiller (1998) was augmented by implementing a new force recovery technique and comprehensive cyclic constitutive rules of the steel tube and concrete core.

A mixed finite element approach following the Hellinger-Reissner variational principle (Zienkiewicz, 1977) was employed in calculating internal forces in an incremental nonlinear analysis. Adopting a mixed formulation allows better representation of inelastic curvatures since independent approximations are introduced for element internal forces and displacements. Linear force shape functions estimate the distribution of bending moment along the element length accurately. Therefore, mixed finite element formulations promise better correlation with fewer elements for problems experiencing inelastic curvatures. In addition, interpolation of element internal loads imposes equilibrium along the element length. This alleviates potential numerical problems due to concrete cracking in displacement-based formulations while enforcing equilibrium (Hajjar & Schiller, 1998). The state determination procedure developed by Alemdar & White (2005) was adopted. Element stiffness and internal forces were formulated within a corotational framework.

In this updated Lagrangian formulation, the variables are defined with respect to the most converged configuration. Based on the principle of virtual displacements, the equilibrium equation can be expressed as given in Equation (2) following the nomenclature by Yang & Kuo (1994), in which the left subscript designates the reference state at which the quantity is measured and the left superscript designates the state at which the quantity takes place. The Hellinger-Reissner mixed formulation is based on introducing force values as variables into the potential energy functional using the Lagrange Multiplier method (Hellinger & Reddy, 1988). Taking the first variation of the modified form of the potential energy functional with respect to force and displacements results in element equilibrium and compatibility equations as given in Equations (2) and (3),

respectively. Both of these equations need to be solved simultaneously within each load increment of a Newton-Raphson solution scheme at the global level. The second integral in the equilibrium equation accounts for the energy due to slip between the steel tube and concrete core (Alemdar, 2001).

$$\int_{1L}^2 D \times \delta_1^2 \hat{d}^T \times dx + \int_{1L}^2 D_{sc} \times \delta_1^2 \hat{d}_{sc}^T \times dx - {}_1^2 Q_{ext} \times \delta_1^2 q^T = 0 \quad (2)$$

$$\int_{1L}^2 ({}_1^2 \hat{d} - {}_1^2 d) \times \delta_1^2 D^T \times dx = 0 \quad (3)$$

In these equations,  $D$  represents the generalized stress resultant cross-section forces including bending moment and axial force terms.  $\hat{d}$  is the generalized cross-section strain calculated from nodal displacements, while  $d$  is the generalized cross-section strain calculated from stress resultant force fields. Curvatures were defined as second derivatives of transverse displacement fields and Green-Lagrange strain was adopted in the axial direction. In Equation (2),  $\hat{d}_{sc}$  is the generalized strain at the steel and concrete interface,  $D_{sc}$  is generalized stress resultant of the steel and concrete interface,  $Q_{ext}$  is the externally applied load, and  $q$  is the nodal displacement vector.

In addition to the element equilibrium and compatibility equations, cross-section equilibrium at each Gauss point along the element length also needs to be satisfied at each load increment such that stress-resultant cross-section forces calculated from the cross-section strains through numerical integration of stresses ( $D_{\Sigma}$ ) should be equal to the cross-section resultants obtained from interpolated forces as given in Equation (4):

$${}_1^2 D - {}_1^2 D_{\Sigma} = 0 \quad (4)$$

The proposed mixed finite element has 12 deformational degrees of freedom in natural coordinates including separate axial ( $u^c, u^s$ ) and rotational degrees of freedom ( $\theta_{zi}^c, \theta_{yi}^c, \theta_{zj}^c, \theta_{yj}^c, \theta_{zi}^s, \theta_{yi}^s, \theta_{zj}^s, \theta_{yj}^s$ ) for the steel tube and concrete core. In addition, two independent axial degrees of freedom at the mid-node ( $u_m^c, u_m^s$ ) were introduced. Cubic Hermitian shape functions were utilized for rotations while quadratic shape functions were employed for the axial deformations, which required the extra degrees-of-freedom at the mid-length.

The forces that are energy equivalent to the natural degrees of freedom were selected such that independent bending moment ( $M_{zi}^c, M_{yi}^c, M_{zj}^c, M_{yj}^c, M_{zi}^s, M_{yi}^s, M_{zj}^s, M_{yj}^s$ ) and axial force ( $P_i^c, P_j^c, P_i^s, P_j^s$ ) values of the steel tube and concrete core were defined at both ends. Linear shape functions were adopted for both the bending moments and axial forces. However, additional transverse displacement

terms were added to the linear bending moment shape function to account for  $P$ - $\delta$  effects (Alemdar & White, 2005). Defining separate bending moment values for the steel tube and concrete core in natural coordinates resulted in calculation of separate shear forces in the local coordinates. Linear distribution of the axial forces is also compatible with the load transfer between the steel tube and concrete core due to the initiation of slip. The torsional response of RCFT members was assumed to be linear elastic. Therefore, torsional degrees of freedoms and forces were excluded from the nonlinear force recovery.

The force recovery procedure is completed in four different stages assuming the analysis proceeds from  $j^{\text{th}}$  iteration to the  $j+1^{\text{th}}$  iteration of a load step:

- 1 Solve for incremental nodal displacements ( $\Delta q$ ) corresponding to the incremental load vector

$$K_t^j \cdot \Delta q^{j+1} = Q_{ext}^{j+1} - R^j \quad (5)$$

- 2 Calculate incremental nodal loads ( $\Delta Q$ ) by multiplying element flexibility ( $H_{11}$ ) with the compatibility equation ( $V$ )

$$\Delta Q = (H_{11}^j)^{-1} \cdot V^j \quad (6a)$$

where:

$$V^j = \int_0^L N_{D1}^T \cdot [\hat{d}^{j+1} - d^j - f^j \cdot (D(Q^j) - D_\Sigma(d^j))] \cdot dx \quad (6b)$$

$$H_{11}^j = \int_0^L N_{D1}^T \cdot f^j \cdot N_{D1}^j \cdot dx \quad (6c)$$

- 3 Solve for incremental cross-section strains ( $\Delta d$ ) from the unbalance of the cross-section equilibrium and cross-section flexibility ( $f$ )

$$\Delta d = f^j \cdot (D(Q^{j+1}) - D_\Sigma(d^j)) \quad (7)$$

- 4 Calculate internal forces ( $R^{j+1}$ )

$$R^{j+1} = (G^{j+1})^T \cdot Q^{j+1} + (G_{sc}^{j+1})^T \cdot q^{j+1} + (G^{j+1} + M_d^{j+1} - H_{12}^{j+1})^T \cdot (H^{j+1})^{-1} \cdot \left[ \int_0^L (N_{D1}^{j+1})^T \cdot [\hat{d}^{j+1} - d^{j+1} - f^{j+1} \cdot (D(Q^{j+1}) - D_\Sigma(d^{j+1}))] \cdot dx \right] \quad (8a)$$

$$G^{j+1} = \int_0^L N_{D1}^{j+1T} \cdot N_{D1}^{j+1} \cdot dx \quad (8b)$$

$$G_{sc}^{j+1} = \int_0^L N_{\delta \hat{d}_{sc}}^{j+1T} \cdot k_{sc}^{j+1} \cdot N_{\delta \hat{d}_{sc}}^{j+1} \cdot dx \quad (8c)$$

$$H_{12}^{j+1} = \int_0^L N_{D1}^{j+1T} \cdot f^{j+1} \cdot N_{D2}^{j+1} \cdot dx \quad (8d)$$

where  $k_{sc}$  is the slip stiffness;  $K_t$  is the tangent stiffness;  $M_d$  is the matrix resulting from linearization of the compatibility equation;  $N_{D1}$  is the shape function matrix for cross-section forces ( $D = N_{D1} \cdot Q$ );  $N_{D2}$  is the matrix resulting from variation of  $D$  ( $\delta N_{D1} \cdot Q = N_{D2} \cdot \delta q$ );  $N_{\delta \hat{d}}$  is the matrix resulting from variation of  $\hat{d}$  ( $\delta \hat{d} = N_{\delta \hat{d}} \cdot q$ ); and  $N_{\delta \hat{d}_{sc}}$  is the matrix resulting from variation of  $\hat{d}_{sc}$  ( $\delta \hat{d}_{sc} = N_{\delta \hat{d}_{sc}} \cdot q$ ).

The accuracy of the analysis is dependent on the constitutive rules selected for steel tube and concrete core. In this research, the cyclic concrete model originally proposed by Chang & Mander (1994) was implemented. Chang & Mander (1994) derived a family of polynomial curves to represent stress vs. strain response of concrete. Envelope curves determine the boundaries of the cyclic response both in tension and compression. Connecting curves define the rule for strain histories between the envelope curves. Transition curves provide set of rules to shift from one connecting curves to the other going in the opposite direction. The original envelope curve recommended by Chang & Mander (1994) was modified by Tort & Hajjar (2004a) based on axially loaded column tests of RCFT members. Typical characteristics of confined concrete in RCFTs were accounted for including residual strength and mild strength degradation (Hajjar et al., 1998). In addition, new sets of connecting and transition rules were derived to account for complex strain histories that might be experienced while conducting nonlinear analysis. For example, unloading capability was added when the strain history is in between the latest unloading point and the target point on the envelope curve as can be seen in Figure 2.

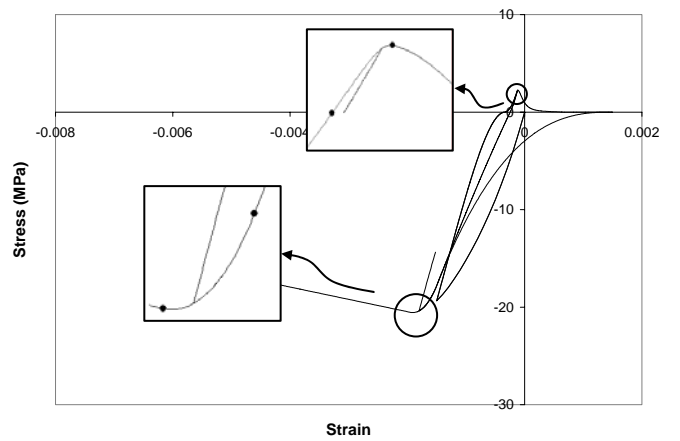


Figure 2. Unloading between the latest unloading point and the target point on the envelope curve

The cyclic constitutive rule of the steel tube was based on a bounding surface uniaxial plasticity model originally developed by Mizuno et al. (1992). An outer bounding surface and an inner loading sur-

face were defined. Plastic loading occurs when stress point breaches the loading surface. Gradual stiffness reduction, the Bauginger effect, reduction of the elastic zone, and the effect of residual stresses due to cold-forming are accounted for in the model. The behavior of steel tube following local buckling was also simulated (Tort & Hajjar, 2004). As can be seen from Figure 3, it was assumed that steel tube attains a negative plastic modulus when the plastic strain limit for local buckling ( $\epsilon_{plb}$ ) is breached.

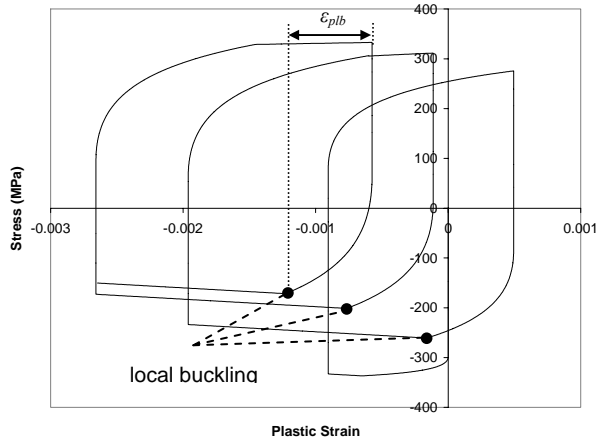


Figure 3. Local buckling of steel tube

#### 4 VERIFICATION STUDIES

The RCFT beam-column element developed in this research was implemented in an open-source analysis framework along with an equivalent steel beam-column element to serve as girders in composite frames (OpenSEES, 1999). Several fully nonlinear verification problems were selected from literature. Two are presented here for brevity.

The first verification problem was a beam-column element tested by Sakino and Tomii (1981) under cyclically applied shear loading and constant axial load (axial load normalized by axial strength  $P/P_o=0.3$ ). The specimen had fixed boundary conditions putting the member into double curvature. The length of the specimen was 600 mm and the steel tube dimensions were  $100 \times 100 \times 2.96$  mm. The measured compressive strength of concrete was 27.0 MPa and the measured yield strength of the steel tube was 298 MPa. The RCFT column was modeled using one finite element. The local buckling strain limit was assumed to be 0.012. Strong correlation was attained between experimental and computational results up to a drift limit of 3% (see Figure 4).

The second verification problem was selected from the tests of Morino et al. (1993) on 3D subassemblies with steel girders framing into an RCFT beam-column in two perpendicular directions (Figure 5). The dimensions of the structural elements can also be seen in Figure 4. The RCFT column was made up of a steel tube with cross-section dimensions of  $125 \times 125 \times 5.74$  mm. The measured compressive strength of concrete was 20 MPa and the

measured yield strength of the steel tube was 395 MPa. The steel girders were all built-up sections with flange and web dimensions of  $125 \times 9$  mm,  $232 \times 6$  mm, respectively. The yield nominal strength of the steel girders was 400 MPa.

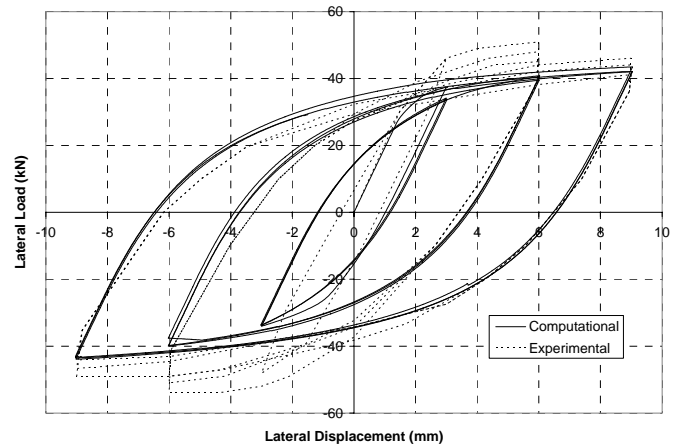


Figure 4. Comparison of experimental and computational results for non-proportionally-loaded RCFT beam-column.

Constant axial load ( $P/P_o=0.15$ ,  $W=21$  kN) was applied on to the pin-pin RCFT column and the steel girder in the Y-Z plane, simultaneously. The top of the RCFT column was left uncapped, allowing slip formation. The steel girder in the X-Z plane was then subjected to cyclic shear loading ( $Q$ ) at both ends. The subassembly was designed such that the RCFT column would sustain damage while steel girders remained elastic.

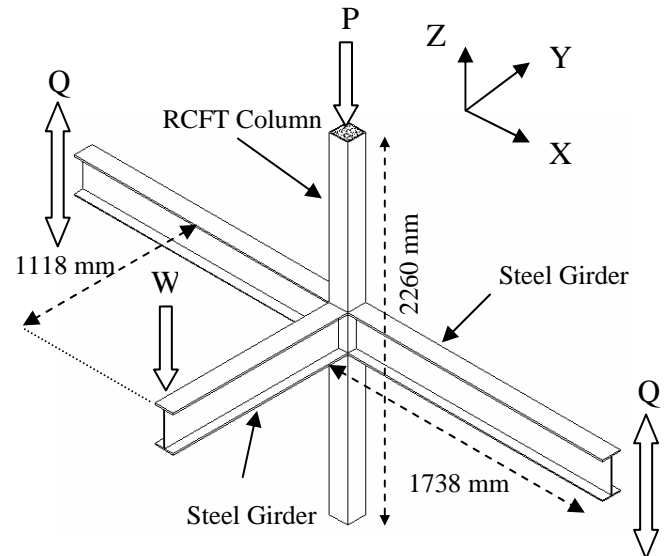


Figure 5. Three-Dimensional RCFT subassembly

The RCFT column and the steel girders in the X-Z were modeled with two elements along the length while the steel girder in the Y-Z plane was modeled with a single element. As can be seen from Figure 6, good agreement was achieved between the experimental and computational results. The amount of slip between steel tube and concrete core was not significant although the bond strength was breached.

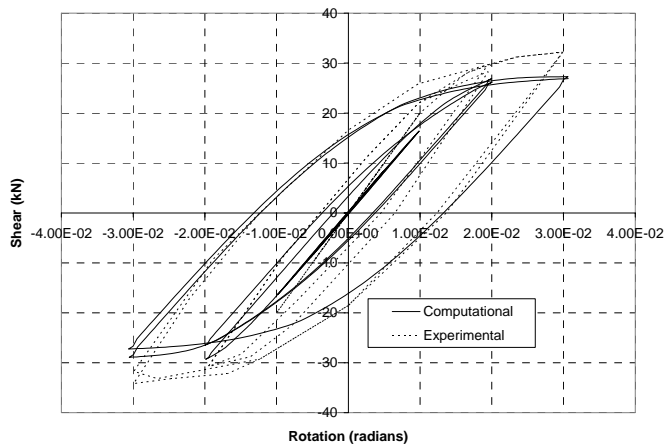


Figure 6. Comparison of experimental and computational results for three-dimensional RCFT subassembly.

## 5 CONCLUSIONS

In this study, research was presented towards evaluating the capacity and demand of RCFT members. These methods were comprehensive enough to investigate various types of engineering demand parameters and damage measures to be used in performance-based design of RCFT structures. The major findings of this research include:

- 1 RCFT members exhibit a wide range of damage states (e.g., concrete cracking, concrete crushing, steel yielding, local buckling, etc.) under both monotonic and cyclic loading. The evolution of the damage states exhibit complex relationships attributed to the composite nature of RCFTs.
- 2 Damage function equations can be used efficiently to quantify the capacity of RCFT members at different performance levels.
- 3 A mixed fiber-based finite element formulation was successfully applied for RCFT columns having slip between the steel tube and concrete core. Strong correlation was achieved for both geometrically and materially nonlinear response.
- 4 The accuracy of distributed plasticity formulation is dependent on the constitutive models. In this research, comprehensive material models were developed accounting for all salient characteristics of RCFT members.
- 5 Future research will focus on using the formulation of this work to conduct parametric studies of multistory RCFT composite frames to quantify their demand and capacity under seismic loading.

## 6 ACKNOWLEDGEMENTS

This research was funded by the National Science Foundation (Grant No. CMS-0084848) and by the University of Minnesota. Any opinions, findings, and conclusions or recommendations expressed in this material are those of the authors and do not reflect the views of the Natl. Science Foundation.

## REFERENCES

- Alemdar, B.N., 2001. *Distributed Plasticity Analysis of Steel Building Structural Systems*. Atlanta, GA: GA Inst. Tech.
- Alemdar, B. N. & White D. W. 2005. Displacement, Flexibility, and Mixed Beam-Column Finite Element Formulations for Distributed Plasticity Analysis. *J. Struct. Eng.* 131(12): 1811-1819.
- Chang, G. A. & Mander, J. B. 1994. *Seismic Energy Based Fatigue Damage Analysis of Bridge Columns: Part I – Evaluation of Seismic Capacity*, Report No. NCEER-94-0006. Buffalo, NY: State University of New York.
- Hajjar, J. F. 2000. Concrete-filled steel tube columns under earthquake loads. *Progress in Structural Engineering and Materials* 2 (1): 72–82.
- Hajjar, J. F., Molodan, A., and Schiller, P. H. 1998. A Distributed Plasticity Model for Cyclic Analysis of Concrete-Filled Steel Tube Beam-Columns and Composite Frames. *Engineering Structures* 20 (4-6): 398-412.
- Heyliger, P. R. & Reddy, J. N. 1988. On a Mixed Finite Element Model for Large Deformation Analysis of Elastic Solids. *Int. J. Non-Linear Mechanics* 23(2): 131-145.
- MacRae, G., Roeder, C. W., Gunderson, C., and Kimura, Y. 2004. Brace-beam-column connections for concentrically braced frames with concrete filled tube columns. *J. Struct. Eng.* 130(2): 233-243.
- Mizuno, E., Shen, C., Tanaka, Y., and Usami, T. 1992. A Uniaxial Stress-Strain Model for Structural Steels under Cyclic Loading. In Y. Fukumoto & G. C. Lee (eds), *Stability and Ductility of Steel Structures Steels under Cyclic Loading*: 37-48. Boca Raton, FL: CRC Press.
- Moehle, J. & Deierlein, G. G. 2004. A Framework Methodology for Performance-Based Earthquake Engineering. Paper No. 679, *Proc., 13<sup>th</sup> World Conf. on Earthq. Engr., Vancouver, BC, Canada, 1-6 August 2004*.
- Morino, S., Kawaguchi, J., Yasuzaki, C., and Kanazawa, S. 1993. Behavior of Concrete-Filled Steel Tubular Three-Dimensional Subassemblages. In W. S. Easterling & W. M. Roddis (eds), *Composite Construction in Steel and Concrete II*: 726-741. New York, NY: Engineering Foundation.
- Morino, S., Uchikoshi, M., and Yamaguchi, I. 2001. Concrete-filled steel tube system-its advantages. *Stl. Struc. I*: 33–44.
- OpenSEES 1999. *Open System For Earthquake Engineering Simulation*. Berkeley, CA: Pacific Earthquake Engineering Research Center, University of California at Berkeley.
- Sakino, K. and Tomii, M. 1981. Hysteretic Behavior of Concrete Filled Square Steel Tubular Beam-Columns Failed in Flexure. *Trans. of the Japan Concrete Institute* 3: 439-469.
- Tort, C. & Hajjar, J. F. 2004. Damage Assessment of Rectangular Concrete-Filled Steel Tubes for Performance-Based Design. *Earthquake Spectra* 20 (4): 1317-1348.
- Tort, C. & Hajjar, J. F. 2004a. Damage Assessment for Performance-Based Design of Rectangular Concrete-Filled Steel Tubes. *Composite Construction in Steel and Concrete V*. Virginia: United Engineering Foundation, American Society of Civil Engineers, in press.
- Yang, Y. B. & Kuo, S. R. 1994. *Theory and Analysis of Nonlinear Framed Structures*. Englewood Cliffs, NJ: Prentice Hall, Inc.
- Yun, S., Hamburger, R. O., Cornell, C. A., and Foutch, D. A. 2002. Seismic performance evaluation for steel moment frames. *J. Struct. Eng.* 128 (4): 534–545.
- Zienkiewicz, O. C. 1977. *The Finite Element Method*. London, UK: McGraw-Hill.